Available online at www.sciencedirect.com
ScienceDirect
Journal of Sound and Vibration 308 (2007) 699–708
JOURNAL OF SOUND AND VIBRATION
www.elsevier.com/locate/jsvi

Stationary and non-stationary vibration of atomising discs

Huajiang Ouyang

Department of Engineering, University of Liverpool, Liverpool L69 3GH, UK

Accepted 22 March 2007
The peer review of this article was organised by the Guest Editor
Available online 30 May 2007

Abstract

This paper presents numerical results of a refined dynamic model for the vibration of atomising discs. The atomising disc is modelled as a thin Kirchhoff plate. Centrifugal and gyroscopic effects of the spinning disc are included in the dynamic model of the disc. As the molten metal spreads out on the disc surface, the inertia force and the self-weight from it as moving loads excite the disc to vibration even if the disc is perfectly symmetric.

The influence of the rotating speed of the disc and the mass flow rate of the metal stream on the dynamics of the disc is investigated. It is shown that the disc motion consists of three stages, a downward deflection, non-stationary vibration and finally stationary vibration with multiple frequencies. The magnitude of motion decreases with increasing disc speed but increases with increasing mass flow rate.

1. Introduction

Discs are a basic mechanical element widely used in engineering. Examples are plentiful and include computer discs, CDs and DVDs, circular saws, disc brakes, turbine discs and so on. Frequently these discs are subjected to loading that moves relative to the discs and are often treated as moving-load problems. Moving loads tend to excite vibration of larger amplitude and/or wider frequency range or higher frequencies and destabilise a dynamic system than conventional non-moving loads.

Mote [1] studied the vibration of a stationary disc subjected to a simple, point-wise rotating load. Iwan and Moeller [2] studied the vibration of a spinning disc subjected to a simple, point-wise stationary load. Ono et al. [3] introduced the follower force and a bending couple to a spinning disc. Ouyang and Mottershead [4] introduced a rotating bending couple due to friction to the vibration of a stationary disc. In addition to the above-mentioned works on disc vibration caused by loading moving in the circumferential direction, Weisensel and Schlack [5] conducted a comprehensive study of the vibration of a stationary disc subjected to radially (as well as circumferentially) moving loads, and Huang and Chiou [6] investigated the vibration of a spinning disc subjected to radially moving loads. Mottershead [7] reviewed a large number of papers on disc vibration excited by moving loads.

Two major types of applications of the moving-load problems of discs have received extensive attention. They are the computer disc problem [3,6,8,9] and the circular wood saw problem [10,11]. Parker [12] and

E-mail address: h.ouyang@liverpool.ac.uk.

0022-460X/$ - see front matter © 2007 Elsevier Ltd. All rights reserved.
doi:10.1016/j.jsv.2007.03.069

Parker and Sathe [13] extended the work on spinning discs to spinning disc-spindle systems. Ouyang et al. [14,15] tackled disc brake vibration and squeal as a moving-load problem.

The vibration of atomising discs was first studied by Ouyang [16]. The disc was modelled as a Kirchhoff plate and the molten metal stream (called melt) as a moving (growing) distributed mass. The initial excitation is supplied by the initial, off-centred impact of the melt descending onto the disc. It was found that the vibration of atomising discs was not stationary with multiple time-dependent frequencies and the transverse vibration of the disc grows in magnitude as the metal stream spreads out on the disc surface. In that model, the melt presents only a growing mass as it spreads out. The growing weight of the mass has been neglected. This is now considered in the current model. In addition, the disc vibration is now excited by the weight of the melt. The data of simulated melt flow [17] are re-fitted. Finally, time-dependent Fourier transform is used to reveal the non-stationary nature of the disc vibration.

2. Centrifugal atomisation

Centrifugal atomisation is carried out in an axial-symmetric enclosure. A schematic view of such a device using a spinning disc is shown in Fig. 1.

The liquid metal (melt) stream flows down from an inlet and drops onto the surface of a flat metal (atomising) disc that is bolted to the shaft through a coupler and spinning at very high speed. The disc may be considered to be clamped at a very small inner radius a. Due to the centrifugal force acting on it, the liquid metal stream is broken into a spray of metal droplets that fly off the disc and become powder particles when cooling down. This is an efficient way of producing high-quality powders. As the melt cools down, part of it gradually solidifies prematurely and accumulates on the disc. As the process goes on, more solid metal accumulates and forms a 'skull' on the disc. The skull hinders the melt flow and droplet flight in the outward radial direction as a barrier and thus reduces yield of powders. The melt on the disc causes it to vibrate. The vibration is rather severe in the case of the centrifugal atomising device at the University of Liverpool.

One shortcoming of Ouyang's [16] study is the assumption of the initial impact that has to be off centred to initiate vibration. If the nozzle is perfectly aligned with the centre of the disc, then the melt will descend onto the centre of the disc and consequently the vibration of the disc cannot be set up by the initial impact assumed in Ref. [16]. As the melt spreads out, it not only adds a growing inertia force to the disc but also applies a growing weight force to the disc. This growing weight will start the vibration in the disc. The whole system has time-dependent growing mass (moving mass) and external load (growing weight force on the disc from the melt).

3. Dynamic model

The metal flow and the formation of the skull on the disc is a complicated process. It depends on the flow rate of the melt, the rotating speed of the disc, the heat transfer coefficient at the liquid–disc interface and the residence time of the melt on the atomising disc, the temperature transfer characteristics and so on [17].

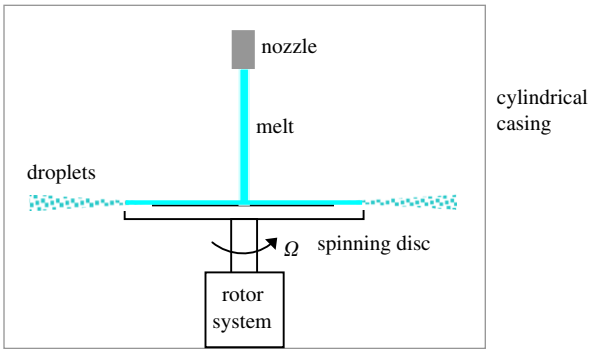

Fig. 1. Schematic diagram of powder production using an atomising disc.

Apparently, a number of physical processes are going on in centrifugal atomisation. The assumptions that must be made in this paper include: (1) there is no thermal and mechanical coupling, (2) the shape and the rate of the melt flow are known a priori, for example, from the simulations of Ref. [17], (3) the melt flow is axial-symmetrical, (4) the melt flow on the disc provides inertia, but no stiffness or damping to the system, (5) there is no interaction between the airflow and the melt flow or between the airflow and the disc vibration and (6) the disc is modelled as a flat, annular, thin (Kirchhoff) plate of equal thickness with clamped-free boundaries. Assumption (3) is largely true at reasonably high mass flow rate. However, a slight deviation from axial symmetry will result in extra excitation and further mathematical complication, which will be considered in future. The interaction mentioned in assumption (5) should exist for an atomising disc spinning at high speeds, as seen from results of other spinning discs [9,18], but is neglected in this paper. By removing any of the above assumptions, the system becomes increasingly complex and more representative of reality.

The disc modelled as a Kirchhoff plate and the melt are shown in Fig. 2 below.

In Fig. 2, $r_m(t)$ and $h_m(r, t)$ are the instantaneous radius and height of the melt. Both vary with time initially and then become steady afterwards. The dashed line represents the surface of melt in liquid state and the solid line the surface of the solidified melt (skull) in solid state. The mechanics of the disc is described in a space-fixed cylindrical coordinate system whose origin is located at the centre of the disc. The radial, circumferential and axial coordinates are denoted by r, θ and z, respectively.

The equation of motion of the disc subjected to an external distributed load p is (adapted from Ref. [2])

$$\rho h\left(\frac{\partial^2 w}{\partial t^2}+2\Omega\frac{\partial^2 w}{\partial t\,\partial\theta}+\Omega^2\frac{\partial^2 w}{\partial\theta^2}\right)+D\nabla^4 w,$$
$$-h\frac{\partial}{r\,\partial r}\left(r\sigma_r\frac{\partial w}{\partial r}\right)-h\frac{\sigma_\theta}{r^2}\frac{\partial^2 w}{\partial\theta^2}=p(r,\theta,t), \tag{1}$$

where ρ, h, D, Ω and p are the mass density, the thickness, the flexural rigidity, the rotating speed and the external distributed load of the disc, and

$$\nabla^4=\left(\frac{\mathrm{d}^2}{\mathrm{d}r^2}+\frac{\mathrm{d}}{r\mathrm{d}r}+\frac{\mathrm{d}^2}{r^2\mathrm{d}\theta^2}\right)^2. \tag{2}$$

The in-plane stresses σ_r and σ_θ in Eq. (1) due to disc rotation [2,3] are:

$$\sigma_r(r)=d_1+\frac{d_2}{r^2}-\frac{3+v}{8}\rho\Omega^2r^2,$$
$$\sigma_\theta=d_1-\frac{d_2}{r^2}-\frac{1+3v}{8}\rho\Omega^2r^2, \tag{3}$$

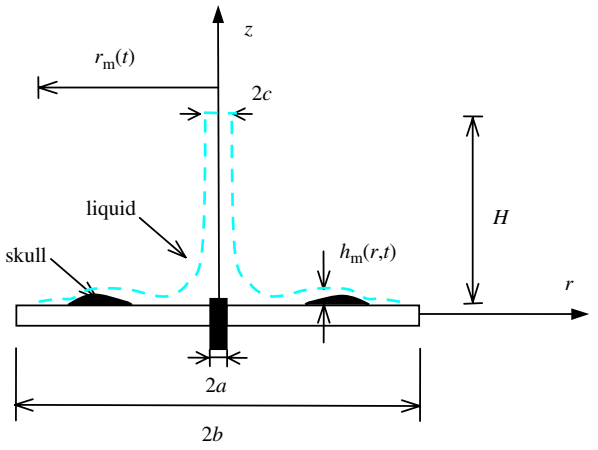

Fig. 2. Dynamic model of the atomising disc.

where

$$d_1 = \frac{1+v}{8}\frac{(v-1)a^4-(3+v)b^4}{(v-1)a^2-(1+v)b^2}\rho\Omega^2,$$
$$d_2 = \frac{1-v}{8}\frac{(1+v)a^2-(3+v)b^2}{(v-1)a^2-(1+v)b^2}\rho\Omega^2 a^2 b^2 \tag{4}$$

and v is the Poisson's ratio of the disc.

In the region where the melt is present on the disc surface, the resultant distributed load has two sources, $-\rho_m(r,t)h_m(r,t)(\partial^2 w/\partial t^2)$ due to the inertia force and $-\rho_m(r,t)h_m(r,t)g$ due to its weight, where ρ_m is the density of the liquid/solid metal on the disc and $g = 9.8\,\mathrm{m\,s^{-2}}$. Hence,

$$p = \begin{cases} -\rho_m(r,t)\left[h_m(r,t)\frac{\partial^2 w}{\partial t^2}+g\right] & a<r\leqslant r_m(t), \\ 0 & r_m(t)<r<b. \end{cases} \tag{5}$$

Suppose that the evolution of the melt flow (the height h_m and radius r_m of the profile) on the disc surface with time is known. Then the distributed load p can be expressed as a function of w and/or its derivative. This information may be obtained through measurement, which is very difficult to conduct owing to various on-going physical processes involved, or through numerical simulations, for example, carried out by Ho and Zhao [17].

The solution of Eq. (1) can be written as

$$w(r,\theta,t) = \sum_{m=0}^{\infty}\sum_{n=-\infty}^{\infty}\phi_{mn}(r,\theta)q_{mn}(t), \tag{6}$$

where the modes of the unloaded disc are:

$$\phi_{mn}(r,\theta) = R_{mn}(r)\mathrm{e}^{\mathrm{i}n\theta}$$
$$(m = 0,\ 1,\ 2,\ \ldots;\ n = 0,\ -1,\ 1,\ -2,\ 2,\ \ldots) \tag{7}$$

As there is no analytical solution for $R_{mn}(r)$, a mathematical function is normally assumed, sometimes with coefficients determined through an energy method or Galerkin's method. Hutton et al. [10] used polynomial functions for $R_{mn}(r)$. Huang and Chiou [6] used 'beam functions' instead and argued that it would be easier to determine the critical speed of the disc. Polynomial functions are selected for $R_{mn}(r)$ of the disc in this paper as [19]

$$R_{mn}(r) = (a_{mn}+b_{mn}r+c_{mn}r^2)(r-a)^{m+2}, \tag{8}$$

where the coefficients a_{mn}, b_{mn} and c_{mn} can be determined at the free boundary of the disc [19]:

$$\left[\left[\frac{\mathrm{d}^2}{\mathrm{d}r^2}+v\left(\frac{\mathrm{d}}{r\,\mathrm{d}r}-\frac{n^2}{r^2}\right)\right]R_{mn}\right]_{r=b} = 0,$$
$$\left[\left[\frac{\mathrm{d}}{\mathrm{d}r}\left(\frac{\mathrm{d}^2}{\mathrm{d}r^2}+\frac{\mathrm{d}}{r\,\mathrm{d}r}-\frac{n^2}{r^2}\right)-(1-v)\frac{n^2}{r^2}\left(\frac{\mathrm{d}}{\mathrm{d}r}-\frac{1}{r}\right)\right]R_{mn}\right]_{r=b} = 0, \tag{9}$$

and the normalisation of

$$R_{mn}(b) = 1. \tag{10}$$

Eq. (9) means that the shear force and the bending moment must vanish at the outer radius of the disc. Eq. (11) is scaling the $R_{mn}(r)$ to unity at the outer radius of the disc. Notice that 'i' in the exponential function in Eq. (7) and subsequent equations stands for $\sqrt{-1}$. The solution of a_{mn}, b_{mn} and c_{mn} is complicated and is determined using a symbolic software package.

4. Numerical solutions

Galerkin's method is usually used to convert the equation of motion of the physical coordinate, Eq. (1), into equations of motion of its modal coordinates. This is done by substituting Eqs. (3)–(6) into (1), multiplying the resultant equation by $\bar{\phi}_{kl}(r,\theta)$ ($k=0,1,2,\ldots$; $l=0,-1,1,-2,2,\ldots$) and then integrating it over the disc area (the bar on top of a symbol represents its complex conjugate). It follows that

$$\begin{aligned}
&\sum_{m=0}^{\infty}\int\left\{\rho h\ddot{q}_{ml}(t)+\mathrm{i}2l\Omega\rho h\dot{q}_{ml}(t)\right.\\
&\left.+q_{ml}(t)\left[D\left(\frac{\mathrm{d}^2}{\mathrm{d}r^2}+\frac{\mathrm{d}}{r\,\mathrm{d}r}-\frac{l^2}{r^2}\right)^2-h\frac{\mathrm{d}}{r\,\mathrm{d}r}\left(r\sigma_r\frac{\mathrm{d}}{\mathrm{d}r}\right)+hl^2\frac{\sigma_\theta}{r^2}\right]\right\}\\
&\times R_{ml}(r)R_{kl}(r)r\,\mathrm{d}r=-\int\left[\rho_{\mathrm{m}}(r,t)h_{\mathrm{m}}(r,t)R_{k0}(r)g+\sum_{m=0}^{\infty}\rho_{\mathrm{m}}(r,t)h_{\mathrm{m}}(r,t)\right.\\
&\left.\times R_{ml}(r)R_{kl}(r)\right]r\,\mathrm{d}r\,(k=0,1,2,\ldots;\ l=0,-1,1,-2,2,\ldots).
\end{aligned}\tag{11}$$

Further mathematical manipulation yields

$$\begin{aligned}
&\sum_{m=0}^{\infty}\left\{[A_{kml}+B_{kml}(t)]\ddot{q}_{ml}(t)+\mathrm{i}C_{kml}\dot{q}_{ml}(t)+F_{kml}q_{ml}(t)\right\}\\
&\quad=f_{k0}(t)(k=0,\ 1,\ 2,\ \ldots;\ l=0,\ -1,\ 1,\ -2,\ 2,\ \ldots),
\end{aligned}\tag{12}$$

where

$$\begin{aligned}
A_{kml}&=\rho h\int_a^b R_{ml}(r)R_{kl}(r)r\,\mathrm{d}r\\
B_{kml}(t)&=\int_a^{r_{\mathrm{m}}(t)}\rho_{\mathrm{m}}(r,t)h_{\mathrm{m}}(r,t)R_{ml}(r)R_{kl}(r)r\,\mathrm{d}r,\\
C_{kml}&=2l\rho\Omega A_{kml},\\
F_{kml}&=\int_a^b\left\{\left[D\left(\frac{\mathrm{d}^2}{\mathrm{d}r^2}+\frac{\mathrm{d}}{r\,\mathrm{d}r}-\frac{l^2}{r^2}\right)^2-h\frac{\mathrm{d}}{r\,\mathrm{d}r}\left(r\sigma_r\frac{\mathrm{d}}{\mathrm{d}r}\right)\right.\right.\\
&\quad\left.\left.-h\frac{\sigma_\theta}{r^2}\frac{\mathrm{d}^2}{\mathrm{d}\theta^2}\right]R_{ml}(r)\right\}R_{kl}(r)r\,\mathrm{d}r,\\
f_{k0}(t)&=-\int\rho_{\mathrm{m}}(r,t)h_{\mathrm{m}}(r,t)gR_{k0}(r)r\,\mathrm{d}r.
\end{aligned}\tag{13}$$

Since $q_{kl}(t)$ is complex, it would be better to replace it with its real part, α_{kl}, and its imaginary part, β_{kl}. In so doing, Eq. (12) becomes

$$\begin{aligned}
&\sum_{m=0}^{\infty}\{[A_{kml}+B_{kml}(t)]\ddot{\alpha}_{ml}(t)-C_{kml}\dot{\beta}_{ml}(t)+F_{kml}\alpha_{ml}(t)\}=f_{k0}(t),\\
&\sum_{m=0}^{\infty}\{[A_{kml}+B_{kml}(t)]\ddot{\beta}_{ml}(t)+C_{kml}\dot{\alpha}_{ml}(t)+F_{kml}\beta_{ml}(t)\}=0.
\end{aligned}\tag{14}$$

A finite number of terms in the infinite series in Eq. (14) are actually needed to arrive at reasonably accurate solutions.

Obviously there is no closed-form solution for Eq. (14), because of $f_{k0}(t)$ and in particular $B_{kml}(t)$. A fourth-order Runge–Kutta algorithm is developed to obtain numerical solutions of Eq. (14) for each retained modal

coordinate. The vibration of the disc is initiated by the melt flowing outward in the radial direction. The initial displacement and velocity of the disc in the z direction are taken to be zero.

Since the mass of the system varies with time, the system does not possess constant frequencies. The non-stationary nature of the system can be characterised by the time-dependent Fourier transform. The time-dependent Fourier transform of a discrete time series $x(k)$ is [20]

$$X(\mathrm{e}^{\mathrm{i}\omega}, n) = \sum_{k=-\infty}^{\infty} x(n-k)W(k)\mathrm{e}^{-\mathrm{i}k\omega}, \tag{15}$$

where $W(k)$ is a suitably chosen window sequence. The display of the magnitude of X as a function of continuous variable ω (vertical axis) and n (horizontal axis representing time) is called a spectrogram [20], which reveals the time-dependent frequency contents in the discrete time series $x(k)$.

The varying 'frequencies' are in the order of hundreds or thousands of radians per second in the present problem. Therefore the time step length in the numerical integration must be very small (in the order of 10^{-5} s). As a result, the computation may take a fairly long time.

5. A numerical example

A real atomising disc is selected for dynamic analysis. The disc is made of pure copper. The material data are taken to be: Young's modulus $E = 130\,\mathrm{GPa}$, Poisson's ratio $v = 0.34$, $\rho = 8920\,\mathrm{kg\,m^{-3}}$. Its geometrical data are $h = 0.003\,\mathrm{m}$, $a = 0\,\mathrm{m}$ (the centre of the disc is clamped), $b = 0.05\,\mathrm{m}$, $c = 0.002\,\mathrm{m}$, $r_0 = 0.003\,\mathrm{m}$. The model metal is titanium. Its density at liquid and solid states is 4100 and $4600\,\mathrm{kg\,m^{-3}}$, respectively. No intermediate values of the density of the modal metal are considered. The mass flow rate $\dot{M}$ may vary. $H = 0.015\,\mathrm{m}$. Most of the above data are taken from Ho and Zhao (2004). Δt is taken to be 2.5×10^{-5} s. Different time step sizes and different number of retained modes are numerically experimented to establish a sufficiently small time step and a sufficient number of retained modes in subsequent computations.

Based on the numerical results reported in Ho and Zhao [17], approximate formulas for h_m, r_m and ρ_m were derived in Ref. [16] and are now (partly) re-fitted in this paper. They are:

$$r_m(t) = \begin{cases} 0.002(1 + 5.33 \times 10^6\, \dot{M} t/\rho_l) & 0 < t < 1.885 \times 10^{-7}\, \rho_l/\dot{M}, \\ 0.004 + (0.01 + 0.0525t + 0.0125t^2) f(\dot{M}) & 1.885 \times 10^{-7}\, \rho_l/\dot{M} \leqslant t, \end{cases}$$

$$\text{At } a \leqslant r < 0.002: \; h_m(r,t) = \begin{cases} 79600\, \dot{M} t/\rho_l & t < 1.885 \times 10^{-7}\, \rho_l/\dot{M}, \\ H & 1.885 \times 10^{-7}\, \rho_l/\dot{M} \leqslant t \leqslant 1, \end{cases}$$

$$\text{at } 0.002 \leqslant r < 0.004: \; h_m(r,t) = \begin{cases} 2.122 \times 10^7\, \dot{M} t(0.004 - r)/\rho_l & t < 1.885 \times 10^{-7}\, \rho_l/\dot{M}, \\ 4(0.004 - r) & 1.885 \times 10^{-7}\, \rho_l/\dot{M} \leqslant t < 1, \end{cases}$$

$$\text{at } 0.01 \leqslant r < r_m < 0.035: \; h_m(r,t) = \left[0.001 + 0.5\sqrt{(r - 0.01)(r_m - r)}\right] \times \{1 - \exp(-0.9t) + 0.32[1 - \exp(-9t)]\} g(\dot{M}) \quad t \leqslant 1,$$

$$\text{at } r > r_m(t): \; h_m(r,t) = 0 \quad t \leqslant 1;$$

$$\text{elsewhere}: \; h_m(t) = 0.002[1 - \exp(-9t)] f(\dot{M}) 1.885 \times 10^{-7}\, \rho_l/\dot{M} \leqslant t \leqslant 1;$$

where

$$f(\dot{M}) = 0.52 + 0.55\dot{M} + 3.5\dot{M}^2,$$

$$g(\dot{M}) = 1.147 - 1.488\dot{M} + 0.178\dot{M}^2.$$

Centrifugal atomisation relies on the centrifugal force produced by the fast rotation of the atomising disc. So the rotational speed Ω is first studied. The vibration of the disc at $(b, 0)$ at three different values of Ω under

a constant mass flow rate of the melt is shown in Fig. 3 (the units of w and t are metres and seconds, respectively).

The flow of the melt on the disc surface consists of three stages: (1) the downward deflection due to the initial descending weight of the melt; (2) growing, non-stationary vibration due to the growing mass and weight as the melt spreads out and gets to the radius of the disc; (3) the steady vibration shortly after the melt reaches the disc radius. These three stages of motion are also present at higher mass flow rates, shown in Figs. 4 and 5. It is also clear that as the disc speed Ω increases, the disc vibration decreases as the centrifugal force is known to be stabilising. This is consistent with Ref. [16].

As the melt spreads out on the disc surface, the total mass of the whole system increases with time. Vibrations in this stage are apparently unsteady. It is expected that the frequencies will decrease with time as a result. In the third stage of vibration, the flow of the melt on the disc becomes steady and it is expected that the

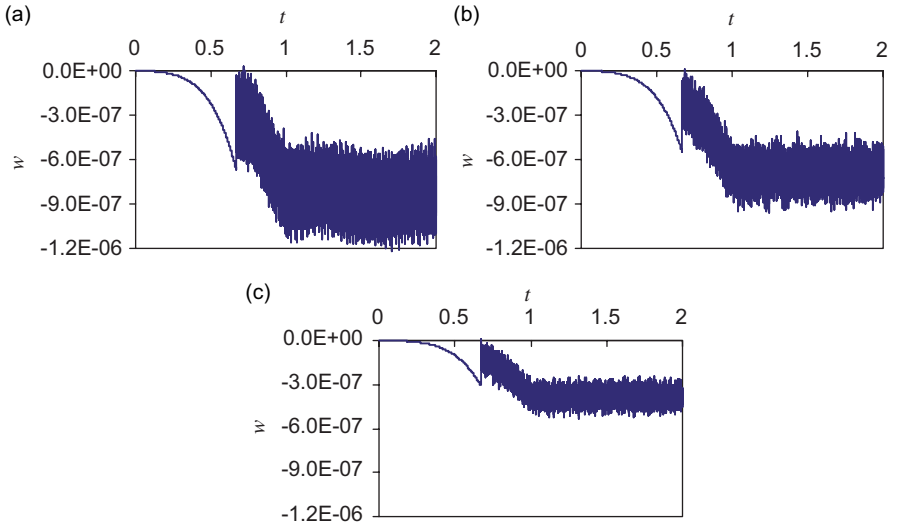

Fig. 3. Disc vibration $w(b,0,t)$ at $\dot{M} = 0.1\,\mathrm{kg\,s^{-1}}$: (a) $\Omega = 0$; (b) $\Omega = 2000\,\mathrm{rad\,s^{-1}}$; and (c) $\Omega = 5000\,\mathrm{rad\,s^{-1}}$.

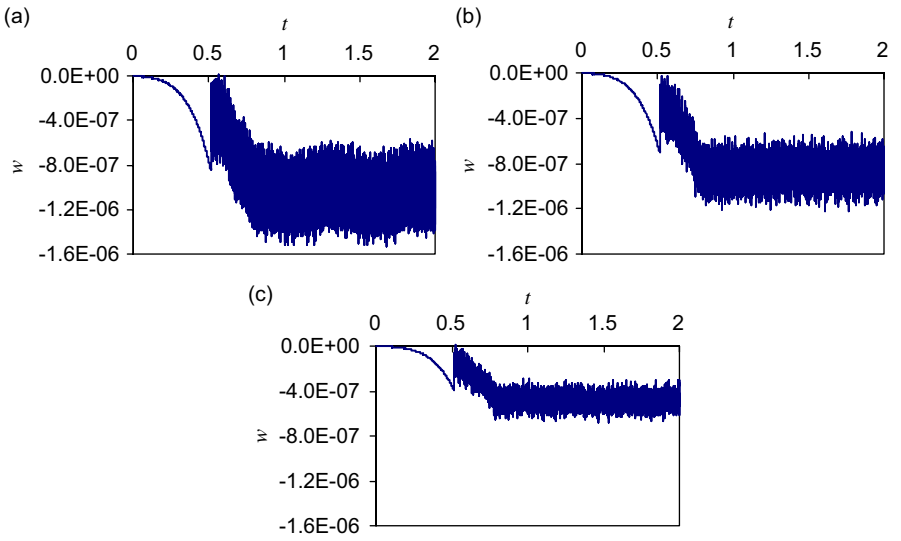

Fig. 4. Disc vibration $w(b,0,t)$ at $\dot{M} = 0.2\,\mathrm{kg\,s^{-1}}$: (a) $\Omega = 0$; (b) $\Omega = 2000\,\mathrm{rad\,s^{-1}}$; and (c) $\Omega = 5000\,\mathrm{rad\,s^{-1}}$.

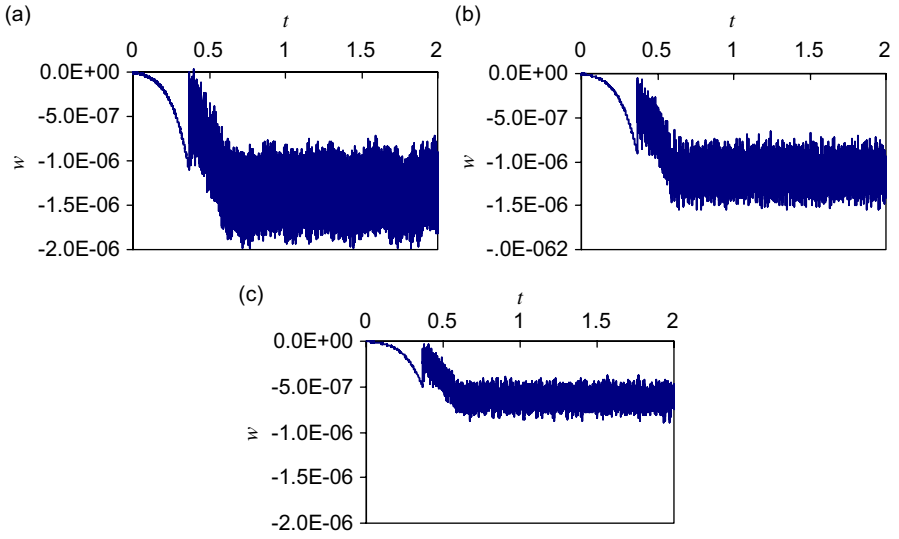

Fig. 5. Disc vibration $w(b,0,t)$ at $\dot{M} = 0.3\,\mathrm{kg\,s^{-1}}$: (a) $\Omega = 0$. (b) $\Omega = 2000\,\mathrm{rad\,s^{-1}}$. (c) $\Omega = 5000\,\mathrm{rad\,s^{-1}}$.

disc vibration will become steady as well. This is demonstrated by the time-dependent Fourier transforms (frequencies in Hz over time in second) of some of the above results in Fig. 6, where the inclined lines with negative gradient (unsteady stage) finally settle to the horizontal lines (steady stage). Notice that there is a line with increasing gradient in each of the plots. But all of them have a tiny contribution to time-domain results (shown in a much lighter colour) and are likely to be a result of numerical integration error. This can be illustrated in Fig. 7 by a conventional Fourier transform to the last 2048 pieces of time-domain data of the numerical results of Fig. 6(d).

Next the mass flow rate of the melt is studied since it influences the flow (skull formation in particular) on the disc [18]. From Figs. 3–5, one can see that the higher the mass flow rate the sooner the second and the third stages of vibration take place, which is expected. It is also clear that the higher the mass flow rate, the greater the vibration magnitude because of the higher weight of the melt acting on the disc in a unit of time. This is also consistent with the finding made in Ref. [16] where the melt descended onto the disc surface as an impact.

It has been noted in Section 3 that the numerical results are obtained based on a number of rather restrictive assumptions, which should be gradually lifted in the subsequent work. There may be more than one course of action. A priority is to include the thermal loading from the melt to the disc and the influence of the temperature on the material properties of the disc. Alternatively, a more accurate plate theory such as Mindlin plate theory or Reissner plate theory may be used to replace the current Kirchhoff plate theory. A third option is to allow mild deviation of axial symmetry of the melt flow and hence introduce a moving load in the circumferential direction (in addition to the moving load in the radial direction). This will add extra mathematical complexity to the dynamic model and should yield more interesting results. An experimental rig of a centrifugal atomisation for the purpose of vibration testing is being designed. Experimental work will be conducted in the near future.

6. Conclusions

The vibration of an annular disc clamped at the inner radius and free at the outer radius subjected to a radially growing, distributed mass is investigated in this paper. This dynamic system is meant to represent the atomising disc in the production of metal powders using centrifugal atomisation. The equation of motion of the dynamic system is derived based on a number of restrictive assumptions. Several findings have been made from the solutions of the equation of motion of the system as follows.

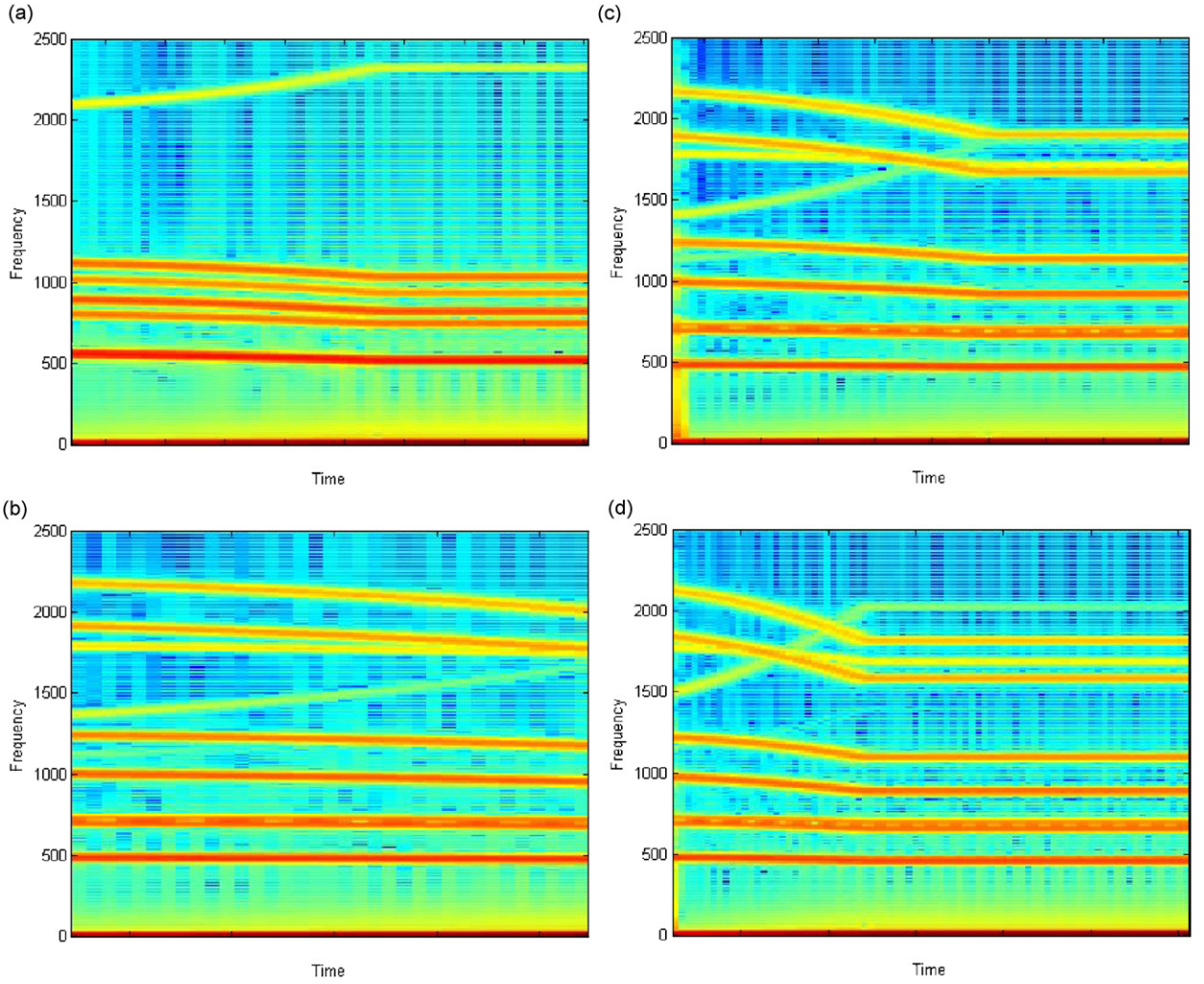

Fig. 6. Time-dependent Fourier transforms (from the beginning of the second stage to 1 second): (a) $\Omega = 0$, $\dot{M} = 0.2\,\mathrm{kg\,s^{-1}}$; (b) $\Omega = 5000\,\mathrm{rad\,s^{-1}}$, $\dot{M} = 0.2\,\mathrm{kg\,s^{-1}}$; (c) $\Omega = 5000\,\mathrm{rad\,s^{-1}}$, $\dot{M} = 0.1\,\mathrm{kg\,s^{-1}}$; (d) $\Omega = 5000\,\mathrm{rad\,s^{-1}}$, $\dot{M} = 0.3\,\mathrm{kg\,s^{-1}}$.

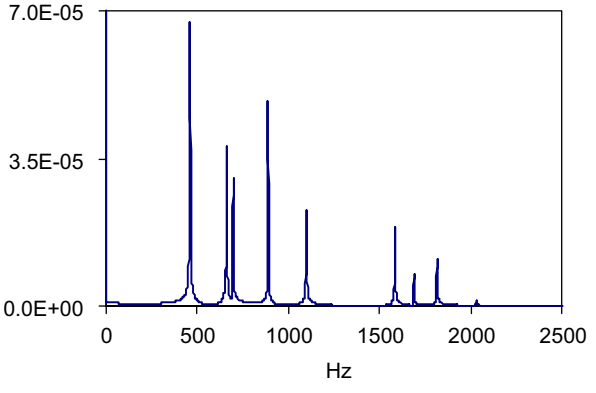

Fig. 7. Fourier transform of steady-state vibration of Fig. 6(d).

(1) The disc motion consists of three stages: a downward deflection, non-stationary vibration and finally stationary vibration.
(2) There are multiple frequencies that decrease with time in the non-stationary stage of vibration.
(3) The disc vibration decreases with increasing disc speed.
(4) The disc vibration increases with increasing mass flow rate of the melt.

Acknowledgement

The author's colleague Dr. Y.Y. Zhao has provided useful information.

References

[1] C.D. Mote Jr., Stability of circular plates subjected to moving loads, *Journal of the Franklin Institute* 290 (1970) 329–344.
[2] W.D. Iwan, T.L. Moeller, The stability of a spinning disc with a transverse load system, *ASME Journal of Applied Mechanics* 43 (1976) 485–490.
[3] K. Ono, J.-S. Chen, D.B. Bogy, Stability analysis of the head-disk interface in a flexible disc drive, *ASME Journal of Applied Mechanics* 58 (1991) 1005–1014.
[4] H. Ouyang, J.E. Mottershead, Dynamic instability of an elastic disc under the action of a rotating friction couple, *ASME Journal of Applied Mechanics* 71 (2004) 753–758.
[5] G.N. Weisensel, A.L. Schlack Jr., Response of annular plates to circumferentially and radially moving loads, *ASME Journal of Applied Mechanics* 60 (1993) 649–661.
[6] S.C. Huang, W.J. Chiou, Modeling and vibration analysis of spinning-disk and moving-head assembly in computer storage systems, *ASME Journal of Vibration and Acoustics* 119 (1997) 185–191.
[7] J.E. Mottershead, Vibration and friction-induced instability in discs, *Shock and Vibration Digest* 30 (1998) 14–31.
[8] R.C. Benson, D.B. Bogy, Deflection of a very flexible spinning disk due to a stationary transverse load, *ASME Journal of Applied Mechanics* 45 (1978) 636–642.
[9] M.H. Hansen, A. Raman, C.D. Mote Jr., Estimation of nonconservative aerodynamic pressure leading to flutter of spinning disks, *Journal of Fluids and Structure* 15 (2001) 39–57.
[10] S.G. Hutton, S. Chonan, B.F. Lehmann, Dynamic response of a guided circular saw, *Journal of Sound Vibration* 112 (1987) 527–539.
[11] J. Tian, S.G. Hutton, Self-excited vibration in flexible rotating discs subjected to various transverse interactive forces—a general approach, *ASME Journal of Applied Mechanics* 66 (1999) 800–805.
[12] R.G. Parker, Analytical vibration of spinning, elastic disk-spindle systems, *ASME Journal of Applied Mechanics* 66 (1999) 218–224.
[13] R.G. Parker, P.J. Sathe, Free vibration and stability of a spinning disk-spindle system, *ASME Journal of Vibration and Acoustics* 121 (1999) 391–396.
[14] H. Ouyang, J.E. Mottershead, D.J. Brookfield, S. James, M.P. Cartmell, A methodology for the determination of dynamic instabilities in a car disc brake, *International Journal of Vehicle Design* 23 (2000) 241–262.
[15] H. Ouyang, J.E. Mottershead, W. Li, A moving-load model for disc-brake stability analysis, *ASME Journal of Vibration and Acoustics* 125 (2003) 53–58.
[16] H. Ouyang, Vibration of an atomising disc subjected to a growing distributed mass, *Journal of the Mechanics and Physics of Solids* 53 (2005) 1000–1014.
[17] K.H. Ho, Y.Y. Zhao, Modelling thermal development of liquid metal flow on rotating disc in centrifugal atomisation, *Materials Science and Engineering A* 365 (2004) 336–340.
[18] A. Jana, A. Raman, Aeroelastic flutter of a disk rotating in an unbounded acoustic medium, *Journal of Sound and Vibration* 289 (2006) 612–631.
[19] J. Chung, J.-E. Oh, H.H. Yoo, Non-linear vibration of a flexible spinning disc with angular acceleration, *Journal of Sound and Vibration* 231 (2000) 375–391.
[20] S.K. Mitra, *Digital Signal Process—A Computer-Based Approach*, second ed, McGraw-Hill, 2001.